Research progress of high precision and selective atomic layer etching technology

OUYANG Yi[1, *], YAN Guanghui[1], CHEN Guoxiang[1], HUANG Gaoshan[1, 2, 3], CHEN Xiangzhong[1, 2, 3], BAO Zhihao[1], SHI Jianjun[1, 2], ZUO Xueqin[3, 4], MEI Yongfeng[1, 2, 3, *]

(1. Yiwu Research Institute, Fudan University, Yiwu 322000, China; 2. International Institute for Intelligent Nanorobots and Nanosystems, Fudan University, Shanghai 200438, China; 3. Department of Materials Science, Fudan University, Shanghai 200438, China; 4. Jiangsu MNT Micro and Nanotech Co., Ltd., Wuxi 214112, China)

Abstract: With the rapid development of semiconductor technology, the critical dimensions of chips continue to shrink. Complex three-dimensional structures represented by fin field-effect transistors (FinFETs) and three-dimensional NAND flash memory have put extremely high demands on the etching process. Traditional dry etching technology is increasingly unable to meet the requirements, especially in terms of high precision, low-damage etching, and achieving etching selectivity between different materials. As a high-precision atomic-scale microfabrication technology, atomic layer etching (ALE) has gradually become one of the key technologies in semiconductor manufacturing. This paper reviews the unique advantages, basic principles, and classification of ALE technology, with a focus on elaborating the ALE processes for different material systems, the application of selective ALE in advanced semiconductor device manufacturing, and the application of ALE in the field of selective deposition.

Key words: atomic layer etching; etching selectivity; isotropic; self-limiting reaction

0 Introduction

Currently, the physical feature sizes of micro-nano electronic devices in advanced integrated circuits have crossed the 10 nm mark. Semiconductor devices based on metal-oxide-semiconductor field-effect transistors (MOSFETs) are gradually approaching their physical limits, posing great challenges to the semiconductor industry[1-2]. The complete integrated circuit manufacturing process is usually divided into front-end wafer fabrication and back-end packaging. Front-end wafer fabrication involves processes such as photoresist coating, exposure, development, etching, thin film deposition, doping, oxidation, diffusion, cleaning, and metrology[3], with complex processes and high requirements for equipment. Among them, etching, photolithography, and thin film deposition are listed as the three core processes in wafer fabrication. The role of etching is to carve out the three-dimensional microstructures required for integrated circuits on the substrate and other

Fund projects: National Natural Science Foundation of China (No. 52201205; No. 12475259; No. 62375054); National Science and Technology Key Project (No. 2021YFA0715302); Shanghai Science and Technology Commission Project (No. 21142200200; No. 22ZR1405000).
Corresponding authors:
Ouyang Yi (1993—), male, Ph.D., young researcher, main research direction is atomic layer etching technology (E-mail: ouyangyi@ywfudan.cn).
Mei Yongfeng (1976—), male, Ph.D., professor, main research direction is nanofilms and micro-nano devices (E-mail: yfm@fudan.edu.cn).

materials on the wafer surface through physical and chemical methods, transferring the mask pattern to the wafer surface. Etching technology has played a crucial role in promoting and continuing Moore's Law, making significant contributions to the reduction of transistor size and the improvement of performance[4].

With the upgrading of integrated circuit processes, high-aspect-ratio and even three-dimensional micro-nano structures (such as fin field-effect transistors (FinFETs) and three-dimensional NAND flash memory) have put higher requirements on existing etching processes. Especially when the feature size is less than 10 nm, the limitations of wet etching in line width control, etching precision, and directionality have gradually become apparent, and it has been gradually replaced by dry etching[5]. Fig. 1 summarizes the development of etching technologies and the characteristics of various methods. With technological progress, dry etching has improved in etching anisotropy and precision, which is conducive to the construction of fine nanostructures. However, within the next 10 years, the acceptable feature size precision of micro-nano electronic devices is expected to reach the order of 3-4 silicon atoms. In addition to geometric precision, the impact of surface defects cannot be ignored, because the surface has become an important part of the device and has a significant impact on its electronic performance[6]. Therefore, there is an urgent need to develop new high-precision etching technologies to meet the growing demands. In the current semiconductor industry, most etching processes require directional material removal, among which the most widely used technology is reactive ion etching (RIE), which belongs to a type of dry etching. In the RIE process, ions and neutral beams are accelerated to bombard the wafer surface to remove the thin film on the surface[7]. During etching, reactive ions interact with electrons, neutral particles, etc., at the reaction interface simultaneously, so RIE is called "continuous" etching[4]. In the continuous etching process, the ions and neutral particles involved in the interface reaction interact with reaction products and substrate atoms, leading to the formation of a mixed layer film at the interface[8]. The existence of this mixed layer may reduce the etching rate, increase surface roughness, or leave non-volatile residues, thereby reducing etching precision[7-9].

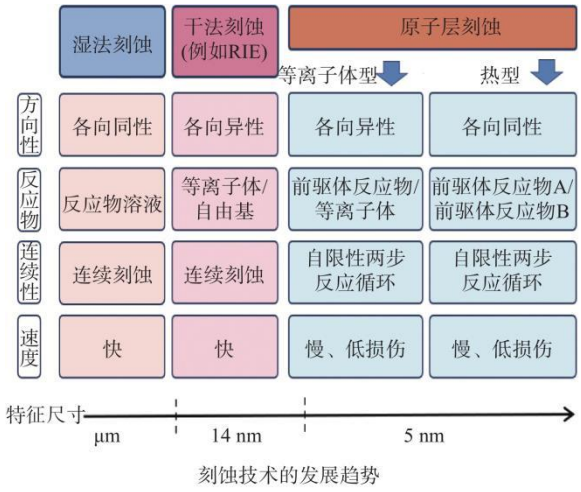

Fig. 1 Development trend and characteristics of etching technology

The Bosch process avoids the drawbacks of continuous etching by alternately switching etching gas and passivation gas, using a periodic "etching-passivation-etching" cycle[10], but it still cannot solve the problems of low etching precision, high surface roughness, and insufficient etching selectivity. As the thickness of thin films in advanced nanodevices approaches 2-3 nm, how to achieve atomic layer-scale etching precision control, improve the etching selectivity of different materials, and obtain low-damage and low-roughness surfaces have become key issues that need to be solved urgently in future etching technologies.

Atomic layer etching (ALE) technology is an advanced etching method that can meet the above requirements. As a technology with atomic layer-level etching precision, ALE can be combined with atomic layer deposition (ALD) to achieve "atomic-level manufacturing". This paper mainly introduces the unique advantages of ALE technology compared with existing dry etching technologies, the principles and classification of ALE in different material systems, and its applications in selective etching of complex nanostructures and area-selective deposition. At the same time, the following issues are focused on: (1) How to use self-limiting reactions to achieve high-precision etching of different materials; (2) How to achieve etching selectivity between different materials; (3) The combination of ALE technology and ALD technology and their applications.

1 Principles and classification of ALE

Initially, ALE was implemented on commercial RIE platforms[11], representing a specialized process window that weakens surface atom-substrate bonds for near-monolayer removal. After three decades of development, ALE's fundamental principles, reaction characteristics, technical routes, and applications have been extensively studied. This section systematically reviews ALE's principles and classifications.

1.1 Principles of ALE

A typical ALE process comprises two half-reactions (Fig. 2)[12]: Half-reaction A modifies the topmost atomic layer using a first precursor to weaken its bonding to the substrate; Half-reaction B either reacts with the modified layer to form volatile products (thermal ALE) or bombards it with ions/neutrals (plasma-enhanced ALE), exposing the next layer. Cyclic execution of these half-reactions enables atomic-scale layer-by-layer etching with precise control[13]. A purge step between half-reactions removes excess reactants and byproducts.

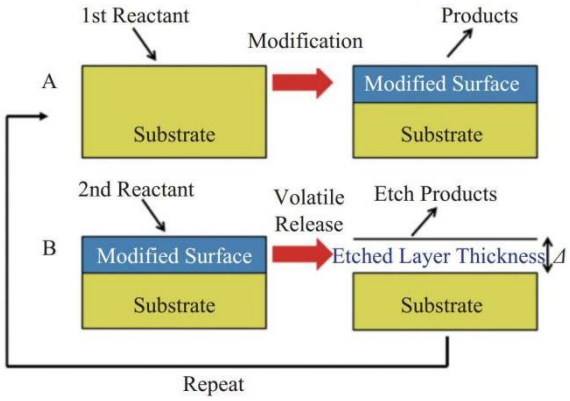

Fig. 2 Schematic diagram of ALE process based on sequential self-limited surface modification and volatile release reactions[12]

The biggest difference between ALE technology and continuous etching technologies such as RIE is that ALE decomposes the continuous etching process into at least two half-reactions with self-limiting properties[11]: For thermal ALE, the etching process consists of two or more interface chemical reactions[14-15]; for plasma-based ALE, the surface modification and physical bombardment steps are independent, which is significantly different from the process in RIE where chemical etching and physical etching act synergistically[6, 16]. The separation between the two half-reactions helps eliminate mutual interference between the surface modification and modified layer removal steps, controls the order of surface reactions, enables self-limiting reactions, and avoids the interface mixed layer formed in continuous RIE and the resulting uncontrollable etching effects[17]. In self-limiting reactions, the precursor only reacts with the outermost atoms of the material, limiting the etching thickness to the range of several atomic layers[18], significantly improving etching precision and helping to obtain high-quality, low-damage flat

surfaces[19]. Therefore, ALE technology shows unique advantages in achieving ultra-fine pattern transfer, high-aspect-ratio etching, and high-quality etched surface preparation[20].

1.2 Classification of ALE technology

Based on different modified layer removal methods, ALE can be divided into thermal ALE and plasma-based ALE. For different material types, the mechanisms of thermal ALE mainly include ligand exchange (Al_2O_3, HfO_2, ZrO_3, AlN, AlF_3), conversion reaction (SiO_2, ZnO, WO_3, TiO_2), oxidation and fluorination reactions (TiN, W), etc.[12, 17]. This technology can achieve high etching precision while achieving a high etching selectivity ratio between different materials. In addition, since it consists entirely of gas-phase chemical reactions, thermal ALE has isotropic characteristics[14]. The most widely used method in plasma-based ALE is to reduce the bonding force between the outermost atoms of the thin film to be etched and the matrix through surface chlorination or fluorination, and then use low-energy Ar^+ ions or neutral beams to bombard and remove the modified layer[21]. For example, in the etching process of silicon thin films, chlorine gas is first introduced to generate Si—Cl bonds (4.2 eV) on the wafer surface. The charge transfer effect reduces the Si—Si bonding energy under the $SiCl_x$ layer from 3.4 eV to 2.3 eV[22-23], thus forming a process window (2.3-3.4 eV) for removing the surface modified layer. The plasma bombardment energy required to remove the modified layer is much lower than that of RIE, which can ensure better surface quality and lower damage. In addition, the generation of interface mixed layers is avoided in the separated two-step reaction, making the reaction more stable and controllable[11]. At the same time, the anisotropic etching ability makes plasma-enhanced ALE more suitable for etching high-aspect-ratio nanostructures[4].

2 Development history of ALE technology

The early development of ALE technology can be regarded as an exploration of alternatives to RIE, so plasma-based ALE technology was developed initially. Fig. 3 shows important development nodes of ALE technology. The earliest ALE technology was first proposed by Yoder[24] in 1988. By modifying diamond films with nitrogen oxides and using rare gas ion bombardment to remove the outermost atoms of the film, they achieved atomic layer etching and applied for a US patent. Another early study was the "bilayer etching" of gallium arsenide using chlorine chemisorption reported in 1989[25]. In 1990, Horiike et al.[26] were the first to carry out research on the silicon ALE process. They limited the spontaneous etching of the wafer at −60 ℃, and realized atomic layer etching on the wafer surface by fluorinating the wafer surface with CF_4 plasma and removing the modified layer with Ar^+ ions[26]. In 1993, Matsuura et al.[27] achieved self-limiting layer-by-layer etching of silicon through alternating chlorine adsorption and Ar^+ ion bombardment at room temperature. In 2008, Park et al.[28] realized self-limiting etching of high-*k* dielectric layers using BCl_3 adsorption and Ar neutral beams, with an etching rate of 0.12 nm·cycle^{-1}. Studies have shown that compared with RIE, atomic layer etching can avoid the hafnium enrichment on the HfO_2 surface and minimize etching damage[28]. In 2014, the semiconductor manufacturing technology research alliance (SEMATECH) held the first ALE seminar in the United States, attracting extensive attention from academia and industry. In 2016, Lam Research announced that plasma-enhanced ALE dielectric film etching had achieved mass

production of 10 nm logic devices[21]. Up to now, ALE technology has been widely applied to important material systems such as metal oxides, III-V semiconductors, metal nitrides, and metal elements[14, 25-26, 28-35], showing broad application potential in integrated circuits, biomedicine, sensor technology, and other fields.

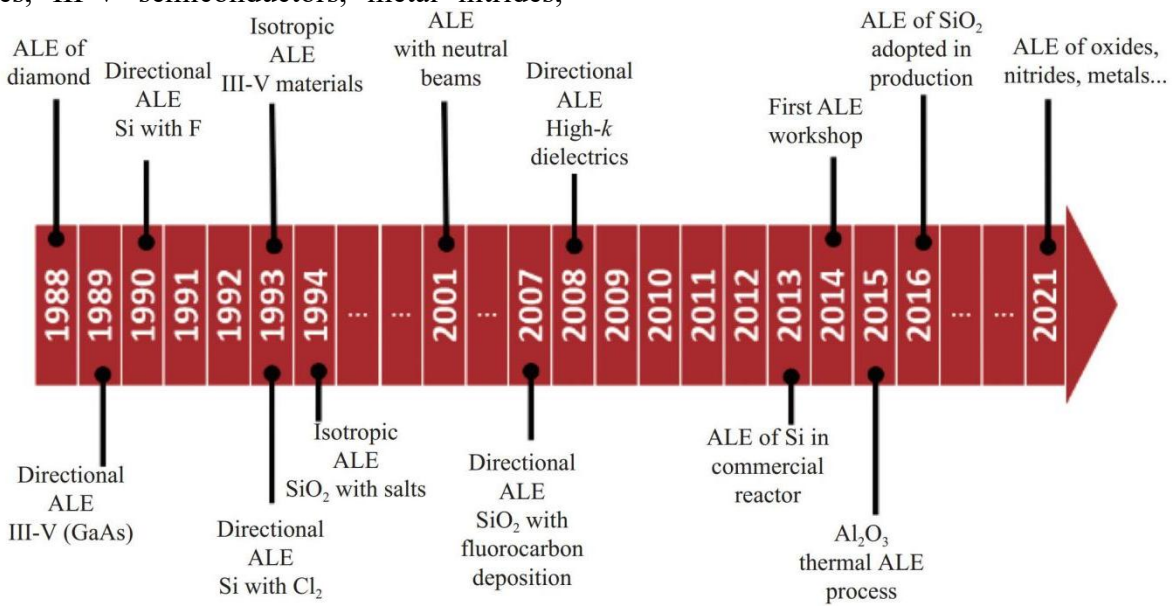

Fig. 3 Development history of atomic layer etching technology

3 Characteristics and applications of ALE technology

The development of ALE processes for different materials is the core of ALE technology development, which helps explore the ALE reaction mechanisms of different material systems and clarify the influence of different reaction parameters on self-limiting characteristics and etching rates. More importantly, researchers can use different ALE mechanisms to achieve selective removal between different materials or selective deposition on different substrate surfaces, making ALE a powerful tool in advanced semiconductor device manufacturing. The following introduces the ALE process principles and applications of several common nanoscale thin film materials.

3.1 ALE processes for silicon and silicon oxide materials

As the cornerstone of the semiconductor industry, the ALE principles and methods of silicon-based materials have been extensively studied. As mentioned earlier, ALE of silicon mainly uses chlorine to react with silicon thin films to generate Si—Cl bonds, reducing the bonding energy of Si—Si bonds under the $SiCl_x$ layer through charge transfer[22-23], thereby weakening the bonding between the outermost Si atoms and the substrate. Studies by Oh et al.[22] have shown that when 50 eV Ar neutral particle beams are used to bombard the wafer surface, only the surface chlorinated layer is removed without sputtering damage to the underlying silicon, finally achieving an etching rate of approximately 0.136 nm·cycle^{-1}, and the etching amount per cycle is equivalent to the thickness of a single atomic layer of (100)-oriented silicon[22]. For the ALE process of SiO_2, since the bonding energy of Si—O bonds (about 6.4 eV) is higher than that of Si—Cl bonds, chlorination reactions are difficult to weaken the Si—O bonding in the SiO_2 surface layer. In

early studies, Flamm et al.[36] found that the bonding of F atoms with SiO_2 only needs to overcome an energy barrier of about 0.163 eV, so fluorination reactions can proceed spontaneously at a reaction pressure of 0.5 Torr (1 Torr ≈ 133.3 Pa). However, studies by Butterbaugh et al.[37] showed that in the plasma-assisted etching of SiO_2, only 1% of the etching is caused by the spontaneous chemical etching of fluorine atoms; in addition, CF_2 and CF_3 radicals have also been confirmed to be unable to continuously etch SiO_2[38], indicating that the modification of SiO_2 surfaces by CF_x has self-limiting properties. Studies by Metzler et al.[39] further found that when using C4F8/Ar plasma to modify the surface of SiO_2 thin films, a layer of CF_x film is deposited on the film surface, which combines with the outermost SiO_2 to form a modified layer, as shown in Fig. 4. In the subsequent modified layer removal step, the energy of Ar^+ ions is between that required for modified layer removal and physical sputtering, finally achieving an etching rate of 0.4 nm·cycle^{-1}. However, for etching processes relying on plasma bombardment, etching damage remains a problem to be solved[40], so thermal ALE processes without plasma participation have become a more attractive option.

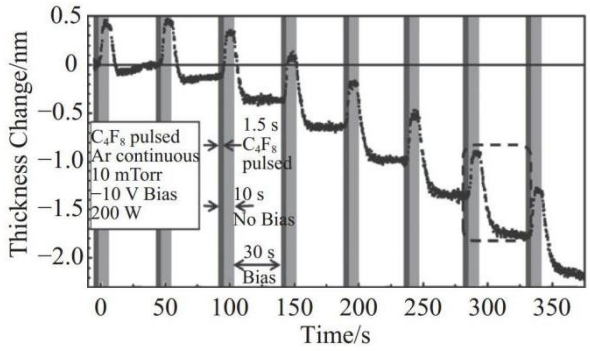

Fig. 4 Thickness variation of SiO_2 film within 8 ALE cycles by a C_4F_8/Ar plasma modification and an Ar plasma sputtering step[39]

In 2017, DuMont et al.[30] reported a method to realize the thermal ALE process of SiO_2 through a "conversion-etch" mechanism. This method converts the outermost SiO_2 into Al_2O_3 and volatile $Si(CH_3)_4$ using $Al(CH_3)_3$. Subsequently, pyridine hydrogen fluoride and $Al(CH_3)_3$ are used to etch the surface Al_2O_3 through fluorination reaction and ligand exchange (the mechanism of Al_2O_3 ALE will be described in detail in the next section). The reason why $Al(CH_3)_3$ can convert SiO_2 is that Al_2O_3 has higher thermodynamic stability than SiO_2. The reaction process[30] is as follows:

$$4Al(CH_3)_3 + 3SiO_2 \rightarrow 2Al_2O_3 + 3Si(CH_3)_4 \quad (1)$$

Calculations using HSC Chemistry software show that at 300 ℃, the Gibbs free energy change of this reaction is $\Delta G = -53.8$ kcal (1 kcal ≈ 4.2 kJ), indicating that the reaction can proceed spontaneously. Fig. 5(a) shows the differential infrared absorption spectra corresponding to SiO_2 after the first reaction with TMA and hydrogen fluoride (HF) at 300 ℃[30]. It can be seen that after the first TMA reaction, the absorption peak intensities of Si—O and Si—OH groups at 975 cm^{-1} and 1250 cm^{-1} weaken, while the absorption peaks of Si—CH_3 groups (at 670 cm^{-1} and 1275 cm^{-1}), Al—CH_3 groups (at 750 cm^{-1} and 1212 cm^{-1}), and Al—O groups (at 845 cm^{-1}) increase[41], which well verifies the above reaction process. In addition, after the reaction with HF (compared with the TMA reaction), the decrease in the absorption peak intensities of Al—O and Si—O—Al groups and the increase in the absorption peak intensities of Si—F and Al—F groups further confirm the fluorination process. As shown in Fig. 5(b), the thermal ALE etching rate of SiO_2 is significantly affected by the reaction pressure. When the reaction pressure reaches 4 Torr, the etching

rate can reach a peak of approximately 0.3 nm·cycle^{-1}[30].

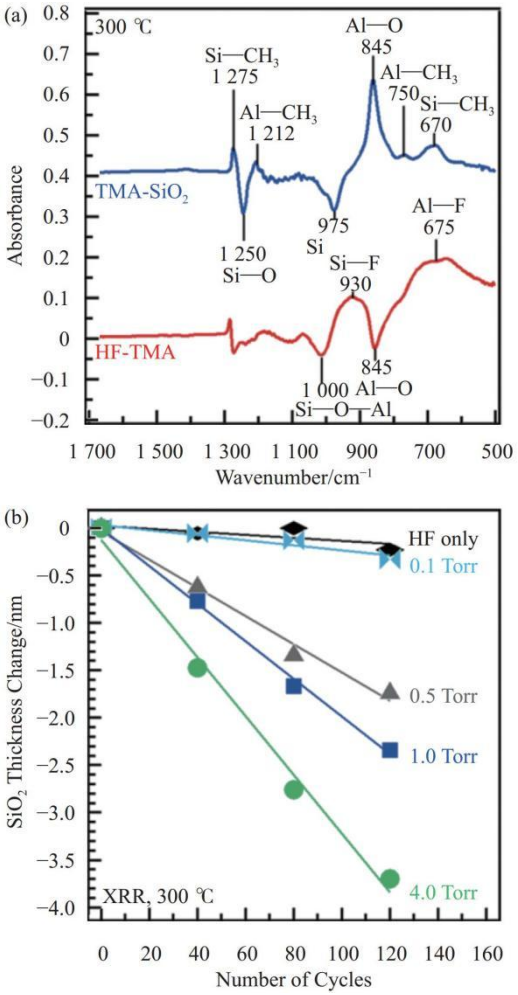

Fig. 5 (a) Difference infrared absorbance spectra during the first TMA and HF exposures on SiO_2 at 300 ℃. (b) SiO_2 film thickness change versus number of ALE cycles at different TMA/HF pressures[30]

3.2 ALE processes for metal oxides

In MOSFETs, the metal oxide layer is usually located between the metal gate and the semiconductor as a gate insulating layer. The material selection and thickness of the oxide layer have important impacts on the performance of MOSFETs. Metal oxides can usually be modified with chlorine to form more stable chlorides, and then the modified layer is removed by Ar^+ ion bombardment. This method can be applied to Al_2O_3[42], HfO_2[43], ZrO_2[44], TiO_2[45], etc. In 2015, the concept of thermal ALE was proposed and first applied to Al_2O_3 ALE, whose principle is shown in Fig. 6(a)[33]. In the thin film surface modification step, pyridine hydrogen fluoride gas reacts with Al_2O_3 to generate AlF_3[33]:

$$Al_2O_3 + 6HF \rightarrow 2AlF_3 + 3H_2O \quad (2)$$

Calculations using HSC Chemistry software show that at 250 ℃, the ΔG of this reaction is −53.8 kcal, indicating that the reaction can proceed spontaneously; in the modified layer removal step, $Sn(acac)_2$ reacts with AlF_3 to generate volatile products $Al(acac)_3$ and SnF(acac), so the total reaction[33] can be expressed as:

$$Al_2O_3 + 6HF + 6Sn(acac)_2 \rightarrow 2Al(acac)_3 + 6SnF(acac) + 3H_2O \quad (3)$$

In thermal ALE processes, fluorination reactions are of great significance because metal oxides are difficult to directly react with precursors to generate volatile products, while metal fluorides (such as AlF_3) can undergo ligand exchange reactions with precursors such as $Al(CH_3)_3$, $AlCl(CH_3)_2$, and $Sn(acac)_2$ to generate volatile products such as $AlF(CH_3)_2$, $AlFCl(CH_3)$, and $Al(acac)_3$[33, 46-47]. In addition, studies by Cano et al.[48] have shown that the reaction between metal oxides and pyridine hydrogen fluoride usually has self-limiting properties, as shown in Fig. 6(b). At 300 ℃, when the reaction pressure of pyridine hydrogen fluoride increases from 1 Torr to 4 Torr, the etching rate increases from approximately 0.2 nm·cycle^{-1} to 0.25 nm·cycle^{-1}; however, the etching rate does not increase linearly with the pressure, but tends to saturate when the pressure reaches about 4 Torr[48]. X-ray photoelectron spectroscopy (XPS) characterization results show that the thickness of the fluoride generated by the reaction between Al_2O_3 and pyridine hydrogen fluoride also shows self-limiting

properties with the change of reaction pressure. At 300 ℃, when the reaction pressure reaches 4 Torr, the thickness of the fluoride is basically stable at about 0.5 nm[48], as shown in Fig. 6(c). Under a given reaction pressure P, the relationship between the fluoride thickness x and the diffusion time t[48] can be expressed as:

$$dx/dt = k_0P/x \quad (4)$$

where k_0 is a constant. Equation (4) indicates that the generated fluoride can act as a diffusion barrier for subsequent reactions, that is, the fluorination reaction has self-limiting properties, which forms the basis for high-precision etching of metal oxides.

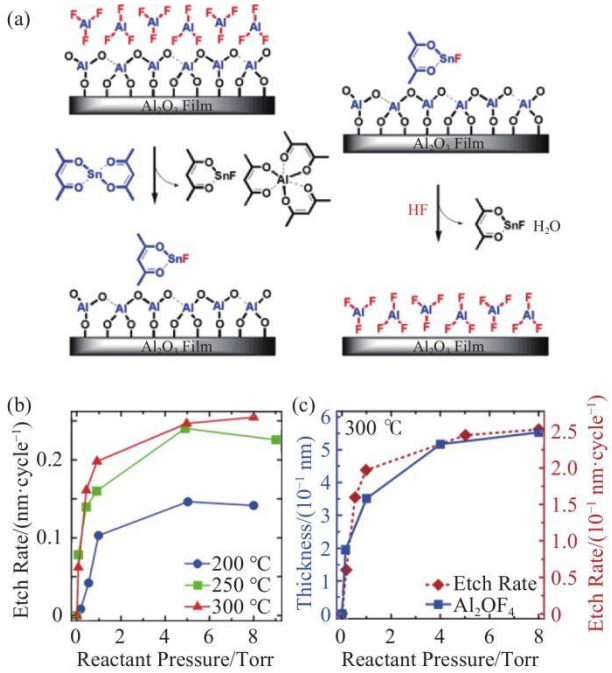

Fig. 6 (a) The reaction of $Sn(acac)_2$ and HF with the Al_2O_3 surface, respectively[33]. (b) The change of etching rate with reaction pressure at different temperatures[33]. (c) The change of fluoride thickness with reaction pressure at 300 ℃[48]

In addition to Al_2O_3, ALE processes for other metal oxides such as ZnO, HfO_2, ZrO_2, TiO_2, and WO_3 have also attracted much attention[31, 34-35, 49]. For ZnO, the precursors for its ALE process can also be $Al(CH_3)_3$ and pyridine hydrogen fluoride. However, different from the ALE process of Al_2O_3, although the product of the fluorination reaction, ZnF_2, can directly react with $Al(CH_3)_3$ to generate volatile $Zn(CH_3)_2$, $Al(CH_3)_3$ can also directly react with the exposed new ZnO surface and convert it into Al_2O_3. The reaction process[35] is as follows:

$$3ZnO + 2Al(CH_3)_3 \rightarrow Al_2O_3 + 3Zn(CH_3)_2 \quad (5)$$

Calculations using HSC Chemistry software show that at 200 ℃, the ΔG of this reaction process is −88.3 kcal, indicating that Al_2O_3 is more stable than ZnO. Therefore, similar to SiO_2, the ALE process of ZnO also uses the "conversion-etch" mechanism, converting it into Al_2O_3 before etching, as shown in Fig. 7[35].

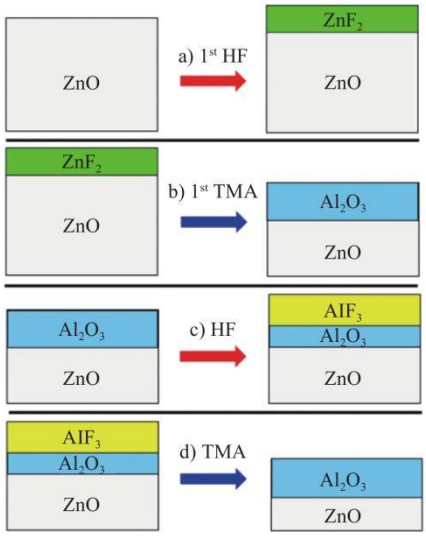

Fig. 7 "Conversion-etch" mechanism of ALE process of ZnO[35]

HfO_2 can undergo ligand exchange reactions with $TiCl_4$[50] or $Sn(acac)_2$[49] after fluorination reaction to generate volatile products $HfCl_4$[50] or $Hf(acac)_4$[49], respectively. However, $Al(CH_3)_3$ cannot undergo ligand exchange with HfF_4 to generate volatile products, nor can it convert HfO_2 through "conversion-etch" for subsequent etching. In contrast, another aluminum-based precursor, $AlCl(CH_3)_2$, can provide additional Cl ligands to combine with

Hf atoms to form stable Hf—Cl bonds, thus realizing the ALE process of HfO_2 through ligand exchange reactions[47]. Similarly, $AlCl(CH_3)_2$ and pyridine hydrogen fluoride can also be used in the ALE process of ZrO_2[47], indicating that it has broader applicability than $Al(CH_3)_3$ and is a universal ALE precursor.

3.3 ALE processes for metal nitrides

TiN is widely used as a diffusion barrier between interconnect metals and dielectric layers in the semiconductor field due to its excellent stability, thermal conductivity, and electrical conductivity[51]. However, studies by Lee et al.[52] have shown that it is difficult to realize ALE of TiN through fluorination and ligand exchange reactions. The reason is that compared with the more stable 4^+ oxidation state, Ti in TiN with a 3^+ valence is difficult to directly generate stable volatile products[51]. Therefore, changing the oxidation state of Ti is particularly important. Ozone (O_3), as a strong oxidant, can oxidize the surface TiN into a TiO_2 modified layer with 4^+ valence Ti. At 200 ℃, the ΔG of this reaction is −184.3 kcal. Investigating the influence of O_3 injection time on the etching rate, it is found that this reaction has self-limiting properties similar to fluorination reactions, as shown in Fig. 8(a)[51]. In the modified layer removal step, pyridine hydrogen fluoride can react with TiO_2 to generate stable volatile product TiF_4. The specific process is as follows:

$$TiN + 3O_3 \rightarrow TiO_2 + NO + 3O_2 \quad (6)$$

$$TiO_2 + 4HF \rightarrow TiF_4 + 2H_2O \quad (7)$$

It is worth noting that although calculations show that the ΔG of reaction (6) at 200 ℃ is 6.9 kcal, experimental results show that HF can etch TiO_2 in the range of 200-300 ℃. A possible explanation is that the reaction does not proceed under steady-state conditions, so the free energy change of the steady-state reaction cannot be used for evaluation. In addition, the by-product H_2O of reaction (7) may play a "autocatalytic" role, further promoting the etching of TiO_2[53]. Studies have also found that temperature has a significant impact on the etching rate, as shown in Fig. 8(b).

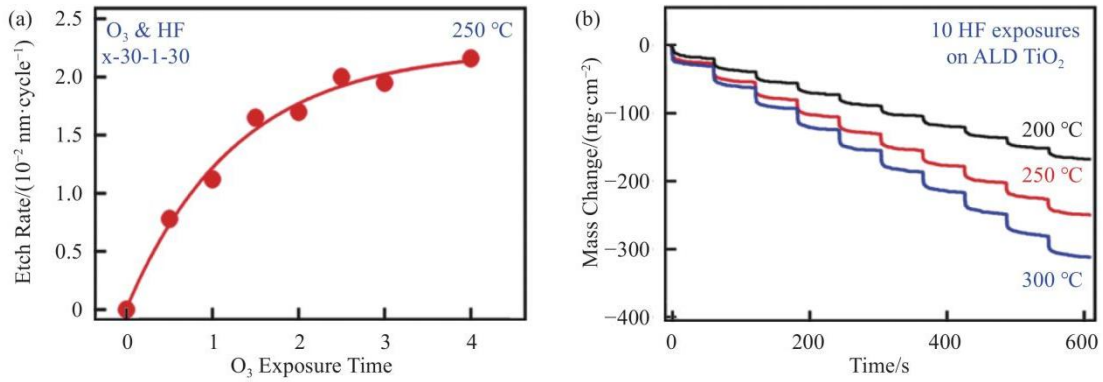

Fig. 8 (a) The self-limiting characteristics of the reaction between O_3 and TiN. (b) The difference in etching rate of TiO2 by HF at different temperatures[51]

In addition to TiN, metal elements in many metal nitrides can be oxidized by ozone to form more stable metal oxides. For example, TaN, NbN, VN, W_2N, Mo_2N, and CrN can be oxidized by O_3 to form more stable metal oxides Ta_2O_5, Nb_2O_5, V_2O_5, WO_3, MoO_3, and CrO_3, which can be further fluorinated to generate volatile compounds TaF_5, NbF_5, VF_5, WF_6, MoF_6, and CrF_6[51]. Thus, it can be seen

that the "oxidation-fluorination" mechanism has wide applicability in ALE of metal nitrides.

3.4 ALE processes for metal elements

Metals play a role in interconnection and filling in semiconductor devices due to their high thermal and electrical conductivity. In recent years, increasing attention has been paid to etching methods for metal elements in the field of integrated circuits. However, due to the corrosion resistance of many metal materials, submicron-scale metal patterning is still very challenging[54]. In this context, ALE technology provides a new feasible path for metal etching.

Similar to ALE of metal nitrides, improving the oxidation state of metals is also crucial for ALE processes of metal elements, because volatile metal complexes are usually in higher oxidation states. For example, for Co and Cu, a common ALE method is to first modify the metal surface with Cl_2 or O_3 to convert them into chlorides with 2^+ or 3^+ valence; then use hexafluoroacetylacetone (Hhfac) to undergo ligand exchange reactions with the chlorides to form volatile metal organic complexes such as $Cu(hfac)_2$[55] and $Co(hfac)_2$[56], thereby realizing precise etching of the metal surface. This method has high selectivity and controllability, enabling precise etching of cobalt and copper materials. In addition to Hhfac, BCl_3 is also used as an important etchant in metal ALE. Especially for W and Mo metals, their ALE processes are realized through the reaction of BCl_3 with metal oxides to generate volatile chlorides[31]. In this process, BCl_3 not only acts as an etchant but also plays a role in surface modification. By precisely controlling the flow rate and reaction time of BCl_3, high-precision etching of W and Mo materials can be achieved[13, 31].

In addition, the use of sulfuryl chloride (SO_2Cl_2) can also cause deoxychlorination of oxidized MoO_3 to generate volatile product MoO_2Cl_2, thereby realizing ALE of Mo[15]. For noble metals, improving their oxidation state is also the key to ALE processes. Akagi et al.[57] used high-density O_2/Ar plasma to oxidize Pt thin films into a modified layer with 4+ valence Pt at a substrate temperature below 80 ℃, and then used formic acid vapor to undergo complexation reactions with the oxide layer to form volatile product $Pt(HCOO)_2$ that can be desorbed from the Pt thin film surface, thereby realizing the ALE process of Pt. The etching rate is 0.3-0.7 nm·cycle^{-1}, and the surface roughness is 0.7-0.9 nm.

ALE processes for metal oxides, nitrides, elements, and silicon-based materials are summarized in Table 1.

Table 1 ALE parameters for different materials

Material	Reactant 1	Reactant 2	Etching rate/ (nm·cycle^{-1})	Temperature/℃	References
Si	CF_4	Ar+	0.136	200	[26]
SiO_2	Cl_2	Ar+	0.064	25	[27]
Al_2O_3	HF	$Sn(acac)_2$	0.061	250	[33]
Al_2O_3	HF	TMA	0.014-0.075	250-325	[46]
HfO_2	HF	$Sn(acac)_2$	0.012	250	[49]
HfO_2	HF	$Al(CH_3)_2Cl$	0.077	250	[52]

ZrO_2	HF	$SiCl_4$/Sn	0.014	350	[52]
ZnO	HF	TMA	0.219	295	[35]
TiO_2	WF_6	BCl_3	0.060-0.070	170	[34]
SiO_2	HF	TMA	0.031	300	[30]
WO_3	BCl_3	HF	0.419	207	[31]
W	O_3/BCl_3	HF	0.250	207	[31]
W	O_2	WF_6	0.630	300	[14]
Mo	O_3	$SOCl_2$	0.094-1.098	75-225	[15]
WSe_2	O_3	KOH	—	25	[29]
TiN	O_3	HF	0.020	250	[51]
AlN	HF	$Sn(acac)_2$	0.036	250	[32]
AlN	HF	$Sn(acac)_2$/H_2 plasma	0.196	250	[32]
AlF_3	HF	$Sn(acac)_2$	0.007-0.063	150-250	[58]

3.5 Applications of selective ALE

Achieving selective etching between different materials is particularly important in the manufacturing process of semiconductor devices[21]. Plasma-based ALE mainly relies on chlorine or fluorocarbons (directly or activated by plasma) to modify thin films, and then uses Ar^+ ions or neutral particles to bombard and remove the modified layer[11], thus lacking "intrinsic" selectivity for different materials. Here, "intrinsic" etching selectivity is defined as: based on a certain mechanism, ALE can only etch specific materials, while having no etching effect on other materials. The key to selective etching in plasma-based ALE is to find ALE windows (such as plasma duration, plasma energy, etc.) for different materials to achieve differences in etching rates between different materials, as shown in Fig. 9[59]. Therefore, most plasma-based ALE is based on "non-intrinsic" selective etching. For example, Li et al.[60] found that due to different reaction pathways for forming volatile etching products, the activation rate of CF_x on the SiO_2 surface is higher than that on the Si_3N_4 surface. Therefore, by reducing the plasma duration, the SiO_2 surface can be completely modified, while the Si_3N_4 surface only partially reacts with CF_x, thereby achieving selective etching of SiO_2 over Si_3N_4[61].

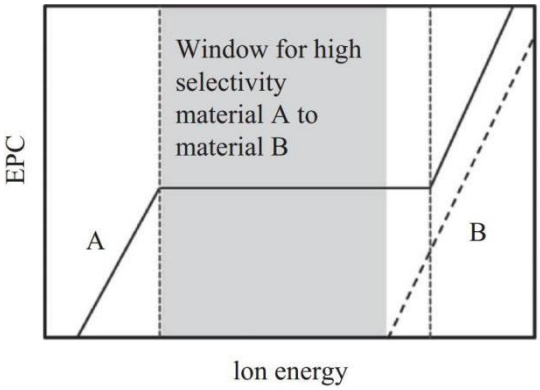

Fig. 9 Schematic of selective ALE achieved by controlling ion energy[59]

On the other hand, the plasma energy required for physical sputtering of Si_3N_4 is generally 20-30 eV[39-40, 60], while that for SiO_2 is about 50 eV[61-64]. Theoretically, in the selective ALE process of SiO_2, the plasma energy should be lower than 20 eV to avoid physical sputtering of Si_3N_4. However, when etching high-aspect-ratio structures, it is usually necessary to increase the plasma energy, which may cause physical

sputtering of Si_3N_4, thereby reducing the SiO_2/Si_3N_4 etching selectivity ratio, or even causing the etching rate of Si_3N_4 to be higher than that of SiO_2[65-66].

With the help of different reaction mechanisms, thermal ALE can more easily achieve "intrinsic" etching selectivity between different materials. For example, studies by Junige et al.[67] have shown that when HF and NH_3 are simultaneously introduced into the reaction chamber at 275 ℃, the etching rate of SiO_2 can reach 0.883 nm·cycle^{-1}, and the etching selectivity ratio of SiO_2 to SiN_x is greater than 1000:1. The main mechanism is that when HF and NH_3 are co-introduced, the etching active species HF_2^- significantly increases the etching rate of SiO_2, while HF_2^- cannot etch SiN_x. Similarly, ALE can also be used for selective etching of nitrides. For example, O_3+HF can etch TiN at 250 ℃, but cannot etch oxides such as ZrO_2, Al_2O_3, HfO_2, and SiO_2, because ZrF_4, AlF_3, and HfF_4 are thermodynamically stable solid products at low temperatures[51], and SiO_2 cannot be directly etched by dry HF[8]. In addition, $Al(CH_3)_3$/HF can effectively etch Al_2O_3, HfO_2, and SiO_2, but cannot etch ZrO_2. The reason is that the ligand exchange product $Zr(CH_3)_4$ of $Al(CH_3)_3$ and ZrF_4 is unstable and decomposes even at a low temperature of 15 ℃, so it cannot effectively remove the ZrF_4 layer on the ZrO_2 surface[52, 68].

It is worth noting that thermal ALE also has the case of "non-intrinsic" selective etching. Under the same reaction mechanism, selective ALE can be realized by utilizing the difference in etching rates. For example, for the InAlAs/InGaAs system, due to the fact that AlAs is more prone to fluorination reaction than GaAs thermodynamically (at 300 ℃, the ΔG of their fluorination reactions is −81.2 kcal and −15.5 kcal, respectively), the etching rate of InAlAs is higher than that of InGaAs [69]. This difference in etching rates can be used to achieve selective etching.

Since thermal ALE can realize high-precision, low-damage, and high-selectivity etching through self-limiting gas-phase reactions without plasma energy participation, it has significant advantages over traditional technologies such as RIE and wet etching in the manufacturing of three-dimensional nanodevices. Especially for extremely fine nanostructures, thermal ALE helps maintain the integrity of the shape and improve surface quality. Lu et al.[69] realized selective thinning of $In_{0.53}Ga_{0.47}As/In_{0.52}Al_{0.48}As$ vertical nanowires using pyridine hydrogen fluoride and $AlCl(CH_3)_2$, further verifying the application potential of ALE in the manufacturing of nanoscale FinFET devices. Fig. 10(a) shows a schematic diagram of the InGaAs n-channel FinFET grown by Molecular Beam Epitaxy (MBE) along the source-drain direction and the Fin cross-sectional direction. Through selective ALE of the InAlAs buffer layer, an InGaAs n-channel with a minimum width of 2.5 nm and an aspect ratio of 20 was released, and 4.7 nm thick Al_2O_3 and W were coated by in-situ ALD to reduce interface oxidation, finally manufacturing InGaAs n-FinFETs with a gate length of only 25 nm, as shown in the transmission electron microscope (TEM) image in Fig. 10(b).

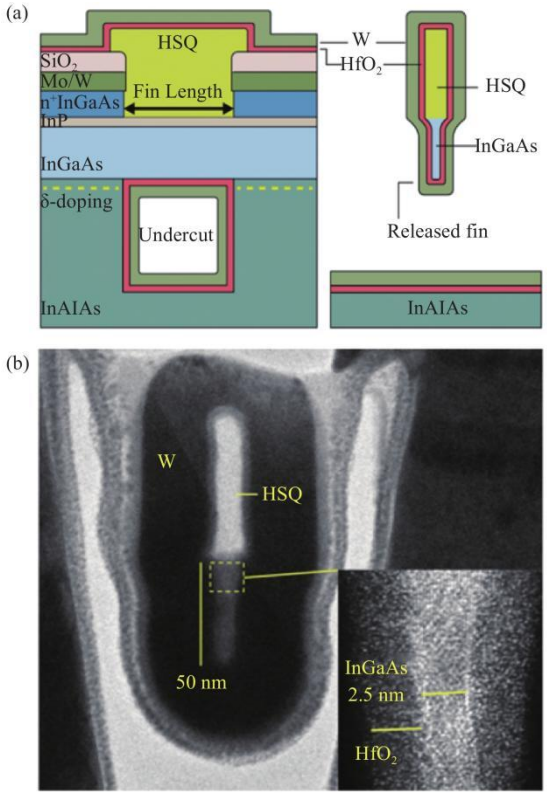

Fig. 10 (a) Cross-sectional schematics along the source-drain direction and across the fin of a InGaAs n-channel FinFET grown by MBE. (b) Cross-section TEM image of a finished FinFET with minimum fin width of 2.5 nm and a highest fin aspect ratio of 20. The inset shows a close-up image of the InGaAs channel[69]

Selective etching also plays an important role in the preparation of nanoring gate structures in gate-all-around (GAA) devices. Li et al.[70] realized selective etching of SiGe over Si using H2O2 and buffered oxide etchant (BOE), and precisely controlled the size of the SiGe channel in SiGe/Si core-shell nanowires using the self-limiting oxidation reaction in the wet etching process (etching rate of 0.5 nm·cycle^{-1}), effectively suppressing the short-channel effect, indicating the potential of ALE in the application of vertical channel devices.

While realizing isotropic and selective etching, ALE can also be used to remove surface defects of compound semiconductors. Edel et al.[71] removed the sputtering damage on the InGaP surface using the self-limiting reaction of HF and TMA, and found that for sputtering damage caused by particles with an energy of 500 eV, the intrinsic properties of the material can be restored after 50 ALE cycles. Auger electron spectroscopy (AES) results show that ALE cycles can remove Ar^+ ions implanted during sputtering, so ALE also has application potential in removing plasma etching damage.

3.6 Area-selective deposition based on ALE

With the reduction of feature sizes of microelectronic devices, traditional top-down processing methods such as photolithography and etching face alignment problems at nodes below 7 nm. Specifically, with the increase in processing steps, subsequent patterning and deposition processes will amplify small deviations in pattern transfer[72-73]. In contrast, Area-Selective Deposition (ASD) adopts a bottom-up method, allowing thin film materials to be deposited only in the desired "growth" areas while minimizing deposition in "non-growth" areas, thereby effectively avoiding the above problems[74]. Early ASD methods mainly achieved selective deposition by introducing film deposition inhibitors in "non-growth" areas, but the inhibitors are prone to failure during cycles, leading to reduced selectivity[75].

In recent years, researchers[72] have proposed combining ALD and ALE technologies to realize a more reliable "atomic-level manufacturing process". For example, studies by Song et al.[76] first proved that ASD without deposition inhibitors can be realized through ALD+ALE supercycles in a single reaction chamber. The principle is shown in Fig. 11[76]. In the ALD process of TiO_2, the thickness of TiO_2 on the Si—OH surface increases linearly with the number of cycles, while there is an obvious nucleation incubation period on the Si—H surface. Etching TiO_2 by ALE during the

incubation period can significantly remove nucleation on the Si—H surface, thereby inhibiting film deposition. Fig. 12 shows TEM and Scanning electron microscope (SEM) images of TiO_2 after ASD. The results show that after 12 ALD+ALE supercycles and 20 ALE cycles, an 8.7 nm thick TiO_2 film is deposited on the Si—OH substrate surface, while only a small amount of particles exist on the Si—H surface, as shown in Fig. 12(a) and (b)[76]. When the number of supercycles increases to 14, the deposition thickness of TiO_2 on the Si—OH substrate can reach 11.8 nm, while the number of particles on the Si—H surface increases but still cannot form a continuous film, as shown in Fig. 12(c) and (d). The above results indicate that constructing ALD+ALE supercycles is a very effective new ASD strategy[73].

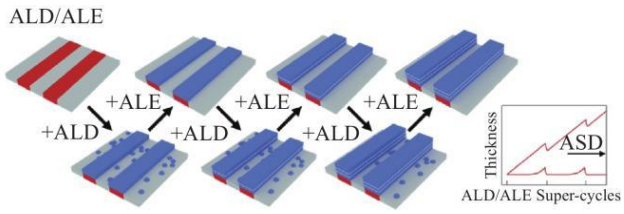

Fig. 11 Schematic diagram of selective deposition of TiO_2 using ALD+ALE super-cycle. The insert shows the thickness variation of TiO_2 deposited on different substrates as the number of ALD+ALE super-cycles increases[76]

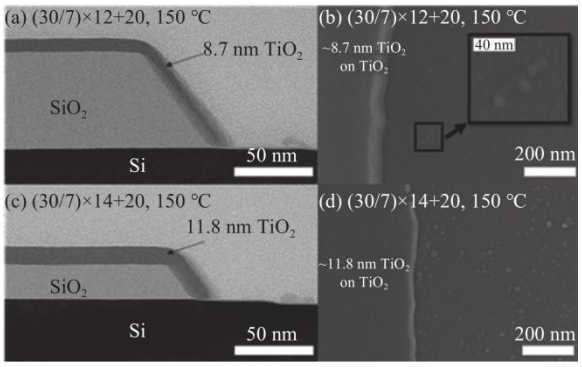

Fig. 12 (a) TEM and (b) SEM images of TiO_2 after 12 ALD+ALE super-cycles and 20 ALE cycles. (c) TEM and (d) SEM images of TiO_2 after 14 ALD+ALE cycles and 20 ALE cycles[76]

In addition to metal oxides, two-dimensional transition metal dichalcogenides have high mobility and unique low-dimensional material properties, which are also important materials in the microelectronics field. Therefore, area-selective deposition technology is also crucial for the fine patterning of such materials. Studies by Soares et al.[75] found that due to the difference in surface hydroxyl concentration, after 20 cycles, the deposition selectivity ratio of MoS_2 on Al_2O_3 and thermally oxidized SiO_2 surfaces is 0.85. However, after performing ALE using MoF_6 and H_2O precursors during deposition intervals, the nucleation of Mo on non-growth areas can be significantly inhibited, increasing the deposition selectivity ratio to 0.95, and achieving more significant selective deposition within a longer ALD cycle range[75]. This further illustrates the wide applicability of the ASD strategy based on ALD+ALE supercycles in different material systems.

4 Conclusions and outlook

The key difference between ALE technology and technologies such as RIE and wet etching is that it decomposes the continuous reaction process into self-limiting thin film surface modification steps and modified layer removal steps, and its unique advantages are reflected in high precision, low damage, and etching selectivity for different materials. At present, plasma-based ALE has been proven to have application potential in fields such as deep silicon etching[77]; while the ligand exchange mechanism involved in thermal ALE can provide a new path for isotropic selective etching, making high-selectivity lateral etching required in 3D chip design for sub-10 nm technology nodes possible[13]. In addition, the method of combining ALD and ALE can improve the deposition selectivity ratio of ASD under high cycle numbers[78], thereby realizing

bottom-up "atomic-level manufacturing". In the future, it is necessary to deeply analyze different ALE mechanisms, realize high-precision, selective etching between various nanoscale thin films, and further verify the feasibility of ALE technology in the manufacturing of advanced devices such as FinFETs, 3D NAND, and GAA[70].

However, the development of ALE technology still faces some challenges: Firstly, the development cycle of ALE processes for different materials is long, and it is difficult to achieve batch development through high-throughput, standardized processes[78]; Secondly, due to its high process complexity, it is still difficult to construct stable and efficient process flows to adapt to large-scale manufacturing[79]. To address the above issues, firstly, in the process development, it is necessary to obtain diverse process data through in-situ characterization methods. Existing solutions include fourier transform infrared spectroscopy (FTIR) [80-81], quartz crystal microbalance (QCM)[67], in-situ ellipsometry[81], quadrupole mass spectrometry (QMS)[82], secondary ion mass spectrometry (SIMS)[70], and optical emission spectroscopy (OES)[83], etc. These methods can provide information such as surface group types, thin film thickness, reaction product types, ion types and concentrations. However, when integrating these detection elements into the ALE reaction chamber, there are still challenges in interface modular design, optimization of gas flow and temperature fields in the chamber, and anti-corrosion treatment of detection elements[83], which require collaboration between semiconductor component suppliers and ALE development teams for customized development. Secondly, it is necessary to use high-precision feedback control methods such as end point (EP) detection and run-to-run (R2R) control to dynamically adjust process parameters during batches and reduce possible interference in actual processes[84]. Finally, based on sufficient process data, construct multi-scale computational models from microscopic molecular dynamics simulation (MDS) and density functional theory (DFT) to macroscopic computational fluid dynamics (CFD)[85-87], and optimize model accuracy through deep learning methods such as recurrent neural networks (RNN) and convolutional neural networks (CNN)[88-90], so as to improve functions in simulation result fitting, natural language processing, etc.[79, 91], ensuring that the model maintains good performance when simulating complex dynamic processes and flow field disturbances in actual manufacturing environments[84]. Ultimately, artificial intelligence can be used to optimize process development or screen process recipes.

In conclusion, the development of ALE technology requires collaboration and iteration in equipment research and development, process development, simulation, and device verification[92]. In the future, ALE will become an indispensable key technology in the field of advanced semiconductor manufacturing.

References:

[1] CHEN Q, WANG L, DUAN X, et al. Investigation of asymmetric characteristics of novel vertical channel-all-around （CAA） In-Ga-Zn-O field effect transistors[J]. IEEE Electron Device Letters, 2022, 43: 894-897.

[2] RATNESH R K, GOEL A, KAUSHIK G, et al. Advancement and challenges in MOSFET scaling[J]. Materials Science in Semiconductor Processing, 2021, 134: 106002.

[3] LAU J H. Recent advances and trends in advanced packaging[J]. IEEE Transactions on

Components, Packaging and Manufacturing Technology, 2022, 12: 228-252.

[4] HUFF M. Recent advances in reactive ion etching and applications of high-aspect-ratio microfabrication[J]. Micromachines, 2021, 12（8）: 991.

[5] RACKA-SZMIDT K, STONIO B, ŻELAZKO J, et al. A review: Inductively coupled plasma reactive ion etching of silicon carbide[J]. Materials, 2021, 15（1）: 123.

[6] OEHRLEIN G S, BRANDSTADTER S M, BRUCE R L, et al. Future of plasma etching for microelectronics: Challenges and opportunities[J]. Journal of Vacuum Science & Technology B, 2024, 42（4）: 041501.

[7] YAMADA S, SAKURAI H, OSADA Y, et al. Formation of highly vertical trenches with rounded corners via inductively coupled plasma reactive ion etching for vertical GaN power devices[J]. Applied Physics Letters, 2021, 118: 102101.

[8] NOS J, ISÉNI S, KOGELSCHATZ M, et al. Cryogenic cyclical etching of Si using CF_4 plasma passivation steps: The role of CF radicals[J]. Applied Physics Letters, 2025, 126（3）: 031602.

[9] TINACBA E J C, ISOBE M, KARAHASHI K, et al. Molecular dynamics simulation of Si and SiO_2 reactive ion etching by fluorine-rich ion species[J]. Surface and Coatings Technology, 2019, 380: 125032.

[10] LAERME F, SCHILP A, FUNK K, et al. Bosch deep silicon etching: Improving uniformity and etch rate for advanced MEMS applications[C]//IEEE International MEMS 99 Conference. Twelfth IEEE International Conference on Micro Electro Mechanical Systems. New York: IEEE, 1999: 211-216.

[11] OEHRLEIN G, METZLER D, LI C. Atomic layer etching at the tipping point: An overview[J]. ECS Journal of Solid State Science and Technology, 2015, 4（6）: N5041-N5053.

[12] GEORGE S M. Mechanisms of thermal atomic layer etching[J]. Accounts of Chemical Research, 2020, 53（6）: 1151-1160.

[13] FISCHER A, ROUTZAHN A, GEORGE S M, et al. Thermal atomic layer etching: A review[J]. Journal of Vacuum Science & Technology A, 2021, 39（3）: 030801.

[14] XIE W, LEMAIRE P C, PARSONS G N. Thermally driven self-limiting atomic layer etching of metallic tungsten using WF_6 and O_2[J]. ACS Applied Materials & Interfaces, 2018, 10（10）: 9147-9154.

[15] NAM T, COLLERAN T A, PARTRIDGE J L, et al. Thermal atomic layer etching of molybdenum using sequential oxidation and deoxychlorination reactions[J]. Chemistry of Materials, 2024, 36（3）: 1449-1458.

[16] TERCERO J U, HIRATA A, ISOBE M, et al. Surface chemical reactions of etch stop prevention in plasma-enhanced atomic layer etching of silicon nitride[J]. Surface and Coatings Technology, 2024, 477: 130365.

[17] FANG C, CAO Y, WU D, et al. Thermal atomic layer etching: Mechanism, materials and prospects[J]. Progress in Natural Science: Materials International, 2018, 28（6）: 667-675.

[18] YOON M Y, YEOM H, KIM J H, et al. Discharge physics and atomic layer etching in Ar/C_4F_6 inductively coupled plasmas with a radio frequency bias[J]. Physics of Plasmas, 2021, 28（6）: 063504.

[19] HONG D, KIM Y, CHAE H. Atomic layer etching of SiO_2 for nanoscale semiconductor devices: A review[J]. Applied Science and Convergence Technology, 2024, 33（1）: 1-6.

[20] SANG X, CHANG J P. Physical and chemical effects in directional atomic layer etching[J]. Journal of Physics D: Applied Physics, 2020, 53（18）: 183001.

[21] KANARIK K, LILL T, HUDSON E, et al. Overview of atomic layer etching in the semiconductor industry[J]. Journal of Vacuum Science & Technology A, 2015, 33（2）: 020802.

[22] OH C K, PARK S D, LEE H C, et al. Surface analysis of atomic-layer-etched silicon by chlorine[J]. Electrochemical and Solid-State Letters, 2007, 10（3）: H94-H97.

[23] SAKURAI S, NAKAYAMA T. Adsorption, diffusion and desorption of Cl atoms on Si（111） surfaces[J]. Journal of Crystal Growth, 2002, 237: 212-216.

[24] YODER M. Atomic layer etching: US4756794[P]. 1988-7-12.

[25] MAKI P, EHRLICH D. Laser bilayer etching of GaAs surfaces[J]. Applied Physics Letters, 1989, 55（2）: 91-93.

[26] HORIIKE Y, TANAKA T, NAKANO M, et al. Digital chemical vapor deposition and etching technologies for semiconductor processing[J]. Journal of Vacuum Science & Technology A, 1990, 8（3）: 1844-1850.

[27] MATSUURA T, MUROTA J, SAWADA Y, et al. Self-limited layer-by-layer etching of Si by alternated chlorine adsorption and Ar^+ ion irradiation[J]. Applied Physics Letters, 1993, 63（20）: 2803-2805.

[28] PARK S, LIM W, PARK B, et al. Precise depth control and low-damage atomic-layer etching of HfO_2 using BCl_3 and Ar neutral beam[J]. Electrochemical and Solid-State Letters, 2008, 11（4）: H71-H73.

[29] NIPANE A, CHOI M S, SEBASTIAN P J, et al. Damage-free atomic layer etch of WSe_2: A platform for fabricating clean two-dimensional devices[J]. ACS Applied Materials & Interfaces, 2020, 13（1）: 1930-1942.

[30] DUMONT J W, MARQUARDT A E, CANO A M, et al. Thermal atomic layer etching of SiO_2 by a “conversion-etch” mechanism using sequential reactions of trimethylaluminum and hydrogen fluoride[J]. ACS Applied Materials & Interfaces, 2017, 9（11）: 10296-10307.

[31] JOHNSON N R, GEORGE S M. WO_3 and W thermal atomic layer etching using “conversion-fluorination” and “oxidation-conversion-fluorination” mechanisms[J]. ACS Applied Materials & Interfaces, 2017, 9（39）: 34435-34447.

[32] JOHNSON N R, SUN H, SHARMA K, et al. Thermal atomic layer etching of crystalline aluminum nitride using sequential, self-limiting hydrogen fluoride and Sn（acac）$_2$ reactions and enhancement by H_2 and Ar plasmas[J]. Journal of Vacuum Science & Technology A, 2016, 34（5）: 050603.

[33] LEE Y, GEORGE S M. Atomic layer etching of Al_2O_3 using sequential, self-limiting thermal reactions with Sn（acac）$_2$ and hydrogen fluoride[J]. ACS Nano, 2015, 9（2）: 2061-2070.

[34] LEMAIRE P C, PARSONS G N. Thermal selective vapor etching of TiO_2: Chemical vapor etching via WF_6 and self-limiting atomic layer etching using WF_6 and BCl_3[J]. Chemistry of Materials, 2017, 29（16）: 6653-6665.

[35] ZYWOTKO D, GEORGE S. Thermal atomic layer etching of ZnO by a “Conversion-Etch” mechanism using sequential exposures of hydrogen fluoride and trimethylaluminum[J]. Chemistry of Materials, 2017, 29（3）: 1183-1191.

[36] FLAMM D, MOGAB C, SKLAVER E. Reaction of fluorine atoms with SiO_2[J]. Journal of Applied Physics, 1979, 50（10）: 6211-6213.

[37] BUTTERBAUGH J, GRAY D, SAWIN H. Plasma-surface interactions in fluorocarbon etching of silicon dioxide[J]. Journal of Vacuum Science & Technology B, 1991, 9（3）: 1461-1470.

[38] INAYOSHI M, ITO M, HORI M, et al. Surface reaction of CF_2 radicals for fluorocarbon film formation in SiO_2/Si selective etching process[J]. Journal of Vacuum Science & Technology A, 1998, 16（1）: 233-238.

[39] METZLER D, BRUCE R L, ENGELMANN S, et al. Fluorocarbon assisted atomic layer etching of SiO_2 using cyclic Ar/C_4F_8 plasma[J]. Journal of Vacuum Science & Technology A, 2014, 32（2）: 020603.

[40] ELGARHY M A I, HAO Q, KIM H, et al. Comparisons of atomic layer etching of silicon in Cl_2 and HBr-containing plasmas[J]. Journal of Vacuum Science & Technology A, 2025, 43（1）: 012601.

[41] FRANK M, CHABAL Y, WILK G. Nucleation and interface formation mechanisms in atomic layer deposition of gate oxides[J]. Applied Physics Letters, 2003, 82（26）: 4758-4760.

[42] MIN K, KANG S, KIM J, et al. Atomic layer etching of Al_2O_3 using BCl_3/Ar for the interface passivation layer of III–V MOS devices[J]. Microelectronic Engineering, 2013, 110: 457-460.

[43] PARK J, LIM W, PARK B, et al. Atomic layer etching of ultra-thin HfO_2 film for gate oxide in MOSFET devices[J]. Journal of Physics D: Applied Physics, 2009, 42（5）: 055202.

[44] LIM W S, PARK J B, PARK J Y, et al. Low

damage atomic layer etching of ZrO_2 by using BCl_3 gas and ar neutral beam[J]. Journal of Nanoscience and Nanotechnology, 2009, 9（12）: 7379-7382.

[45] YEOMÚ G Y. Etch characteristics of TiO_2 etched by using an atomic layer etching technique with BCl_3 gas and an Ar neutral beam[J]. Journal of the Korean Physical Society, 2009, 54（3）: 976-980.

[46] LEE Y, DUMONT J W, GEORGE S M. Trimethylaluminum as the metal precursor for the atomic layer etching of Al_2O_3 using sequential, self-limiting thermal reactions[J]. Chemistry of Materials, 2016, 28（9）: 2994-3003.

[47] LEE Y, GEORGE S M. Thermal atomic layer etching of Al_2O_3, HfO_2, and ZrO_2 using sequential hydrogen fluoride and dimethylaluminum chloride exposures[J]. The Journal of Physical Chemistry C, 2019, 123（30）: 18455-18466.

[48] CANO A M, MARQUARDT A E, DUMONT J W, et al. Effect of HF pressure on thermal Al_2O_3 atomic layer etch rates and Al_2O_3 fluorination[J]. The Journal of Physical Chemistry C, 2019, 123（16）: 10346-10355.

[49] LEE Y, DUMONT J W, GEORGE S M. Atomic layer etching of HfO_2 using sequential, self-limiting thermal reactions with Sn（acac）$_2$ and HF[J]. ECS Journal of Solid State Science and Technology, 2015, 4（6）: N5013-N5022.

[50] LEE Y, GEORGE S M. Thermal atomic layer etching of HfO_2 using HF for fluorination and $TiCl_4$ for ligand-exchange[J]. Journal of Vacuum Science & Technology A, 2018, 36（6）: 061504.

[51] LEE Y, GEORGE S M. Thermal atomic layer etching of titanium nitride using sequential, self-limiting reactions: Oxidation to TiO_2 and fluorination to volatile TiF_4[J]. Chemistry of Materials, 2017, 29（19）: 8202-8210.

[52] LEE Y, HUFFMAN C, GEORGE S M. Selectivity in thermal atomic layer etching using sequential, self-limiting fluorination and ligand-exchange reactions[J]. Chemistry of Materials, 2016, 28（21）: 7657-7665.

[53] JUNG J H, OH H, SHONG B. Fluorination of TiN, TiO_2, and SiO_2 surfaces by HF toward selective atomic layer etching （ ALE ） [J]. Coatings, 2023, 13（2）: 387.

[54] SANG X, XIA Y, SAUTET P, et al. Atomic layer etching of metals with anisotropy, specificity, and selectivity[J]. Journal of Vacuum Science & Technology A, 2020, 38（4）: 043005.

[55] MOHIMI E, CHU X I, TRINH B B, et al. Thermal atomic layer etching of copper by sequential steps involving oxidation and exposure to hexafluoroacetylacetone[J]. ECS Journal of Solid State Science and Technology, 2018, 7（9）: 491-495.

[56] ZHAO J, KONH M, TEPLYAKOV A. Surface chemistry of thermal dry etching of cobalt thin films using hexafluoroacetylacetone （ hfacH ） [J]. Applied Surface Science, 2018, 455: 438-445.

[57] AKAGI D, OKATO T, ISHIKAWA K, et al. Low-temperature atomic layer etching of platinum via sequential wet-like reactions of plasma oxidation and complexation[J]. Applied Surface Science, 2025, 687: 162325.

[58] LEE Y, DUMONT J W, GEORGE S M. Atomic layer etching of AlF_3 using sequential, self-limiting thermal reactions with Sn（acac）$_2$ and hydrogen fluoride[J]. The Journal of Physical Chemistry C, 2015, 119（45）: 25385-25393.

[59] TAN S, YANG W, KANARIK K J, et al. Highly selective directional atomic layer etching of silicon[J]. ECS Journal of Solid State Science and Technology, 2015, 4（6）: N5010.

[60] LI C, METZLER D, LAI C S, et al. Fluorocarbon based atomic layer etching of Si_3N_4 and etching selectivity of SiO_2 over Si_3N_4[J]. Journal of Vacuum Science & Technology A, 2016, 34（4）: 041307.

[61] METZLER D, LI C, LAI C S, et al. Investigation of thin oxide layer removal from Si substrates using an SiO_2 atomic layer etching approach: The importance of the reactivity of the substrate[J]. Journal of Physics D: Applied Physics, 2017, 50（25）: 254006.

[62] DALLORTO S, GOODYEAR A, COOKE M, et al. Atomic layer etching of SiO_2 with Ar and CHF_3 plasmas: A self-limiting process for aspect ratio independent etching[J]. Plasma Processes and Polymers, 2019, 16（9）: 1900051.

[63] DALLORTO S, LORENZON M, SZORNEL J, et al. Balancing ion parameters and fluorocarbon

chemical reactants for SiO_2 pattern transfer control using fluorocarbon-based atomic layer etching[J]. Journal of Vacuum Science & Technology B, 2019, 37（5）: 051805.

[64] METZLER D, LI C, ENGELMANN S, et al. Characterizing fluorocarbon assisted atomic layer etching of Si using cyclic Ar/C_4F_8 and Ar/CHF_3 plasma[J]. The Journal of Chemical Physics, 2017, 146（5）: 052801.

[65] GASVODA R J, ZHANG Z, WANG S, et al. Etch selectivity during plasma-assisted etching of SiO_2 and SiN_x: Transitioning from reactive ion etching to atomic layer etching[J]. Journal of Vacuum Science & Technology A, 2020, 38（5）: 050803.

[66] CHOI M, LEE H, JUNG T, et al. Plasma atomic layer etching of SiO_2 and Si_3N_4 using low global warming hexafluoropropene[J]. Journal of the Korean Physical Society, 2025, 86: 501-511.

[67] JUNIGE M, GEORGE S. Selectivity between SiO_2 and SiN_x during thermal atomic layer etching using Al（CH_3）$_3$/HF and spontaneous etching using HF and effect of HF+ NH_3 codosing[J]. Chemistry of Materials, 2024, 36（14）: 6950-6960.

[68] OH S, LEE S, LEE W J, et al. Rapid extraction of the dielectric constant of atomically thin ZrO_2 prepared through atomic layer deposition and atomic layer etching[J]. Surfaces and Interfaces, 2025, 59: 105911.

[69] LU W, LEE Y, GERTSCH J C, et al. In situ thermal atomic layer etching for sub-5 nm InGaAs multigate MOSFETs[J]. Nano Letters, 2019, 19（8）: 5159-5166.

[70] LI C, ZHU H, ZHANG Y, et al. First demonstration of novel vertical gate-all-around field-effect-transistors featured by self-aligned and replaced high-κ metal gates[J]. Nano Letters, 2021, 21（11）: 4730-4737.

[71] EDEL R, ALEXANDER E, NAM T, et al. Removing defects from sputter damage on InGaP surfaces using thermal atomic layer etching[J]. Journal of Vacuum Science & Technology A, 2024, 42（6）: 062602.

[72] PARSONS G N, CLARK R D. Area-selective deposition: Fundamentals, applications, and future outlook[J]. Chemistry of Materials, 2020, 32（12）: 4920-4953.

[73] CAO K, CAI J, CHEN R. Inherently selective atomic layer deposition and applications[J]. Chemistry of Materials, 2020, 32（6）: 2195-2207.

[74] KIM H, LEE J, LEE S, et al. Area-selective atomic layer deposition of ruthenium using a novel Ru precursor and H_2O as a reactant[J]. Chemistry of Materials, 2021, 33（12）: 4353-4361.

[75] SOARES J, JEN W, HUES J D, et al. Intrinsic and atomic layer etching enhanced area-selective atomic layer deposition of molybdenum disulfide thin films[J]. Journal of Vacuum Science & Technology A, 2023, 41（5）: 052404.

[76] SONG S K, SAARE H, PARSONS G N. Integrated isothermal atomic layer deposition/atomic layer etching supercycles for area-selective deposition of TiO_2[J]. Chemistry of Materials, 2019, 31（13）: 4793-4804.

[77] KIM D S, KIM J B, AHN D W, et al. Atomic layer etching applications in nano-semiconductor device fabrication[J]. Electronic Materials Letters, 2023, 19（5）: 424-441.

[78] KELLER L J, SONG S K, MARGAVIO H R, et al. HfO_2 area selective deposition via substrate-dependent area selective atomic layer etching[J]. Chemistry of Materials, 2025, 37: 1961-1971.

[79] KANARIK K J, OSOWIECKI W T, LU Y, et al. Human-machine collaboration for improving semiconductor process development[J]. Nature, 2023, 616（7958）: 707-711.

[80] HSIAO S N, SEKINE M, HORI M, In situ monitoring of etching characteristic and surface reactions in atomic layer etching of SiN using cyclic CF_4/H_2 and H_2 plasmas [J]. ACS Applied Materials & Interfaces, 2023, 15（29）: 35622-35630.

[81] CHITTOCK N J, MAAS J F W, TEZSEVIN I, et al. Investigation of the atomic layer etching mechanism for Al_2O_3 using hexafluoroacetylacetone and H_2 plasma[J]. Journal of Materials Chemistry C, 2025, 13（3）: 1345-1358.

[82] LII-ROSALES A, JOHNSON V L, SHARMA S, et al. Volatile products from ligand addition of P（CH_3）$_3$ to $NiCl_2$, $PdCl_2$, and $PtCl_2$: pathway for

metal thermal atomic layer etching[J]. The Journal of Physical Chemistry C, 2022, 126（19）: 8287-8295.

[83] LI R, ELICEIRI M H, LI J, et al. Optical emission spectroscopy and gas kinetics of picosecond laser-induced chlorine dissociation for atomic layer etching of silicon[J]. The Journal of Physical Chemistry C, 2025, 129: 2460-2466.

[84] WANG H, OU F, SUHERMAN J, et al. Integration of on-line machine learning-based endpoint control and run-to-run control for an atomic layer etching process[J]. Digital Chemical Engineering, 2025, 14: 100206.

[85] YUN S, TOM M, ORKOULAS G, et al. Multiscale computational fluid dynamics modeling of spatial thermal atomic layer etching[J]. Computers & Chemical Engineering, 2022, 163: 107861.

[86] YUN S, OU F, WANG H, et al. Atomistic-mesoscopic modeling of area-selective thermal atomic layer deposition[J]. Chemical Engineering Research and Design, 2022, 188: 271-286.

[87] ZHUANG L, CORKERY P, LEE D T, et al. Numerical simulation of atomic layer deposition for thin deposit formation in a mesoporous substrate[J]. AIChE Journal, 2021, 67（8）: e17305.

[88] TRIESCHMANN J, VIALETTO L, GERGS T. Machine learning for advancing low-temperature plasma modeling and simulation[J]. Journal of Micro/Nanopatterning, Materials, and Metrology, 2023, 22（4）: 041504.

[89] SUN Q, GE Z. A survey on deep learning for data-driven soft sensors[J]. IEEE Transactions on Industrial Informatics, 2021, 17（9）: 5853-5866.

[90] TOM M, YUN S, WANG H, et al. Machine learning-based run-to-run control of a spatial thermal atomic layer etching reactor[J]. Computers & Chemical Engineering, 2022, 168: 108044.

[91] LEE J, LEE J H, LEE C, et al. Machine learning driven channel thickness optimization in dual-layer oxide thin-film transistors for advanced electrical performance[J]. Advanced Science, 2023, 10（36）: 2303589.

[92] FU H, FU K, YANG C, et al. Selective area regrowth and doping for vertical gallium nitride power devices: Materials challenges and recent progress[J]. Materials Today, 2021, 49: 296-323.